SUPPORTING MATERIALS

	7.0 Tesla		10.5 Tesla	
	1 spoke	**2 spokes**	**1 spoke**	**2 spokes**
Prostate	10.3 – 44.7	13.7 – 44.9	9.2 – 40.7	12.3 – 44.5
Kidneys	10.6 – 43.0	14.5 – 44.6	8.4 – 36.3	11.6 – 43.1
Heart	6.9 – 39.5	9.4 – 43.8	5.7 – 35.4	7.1 – 39.1

Supporting Table S1. Minimum - maximum average flip angle values achieved inside target anatomies using 1- and 2-spoke pulses using 7.0 and 10.5 T antenna arrays. The target flip angle during pulse design was 45°.

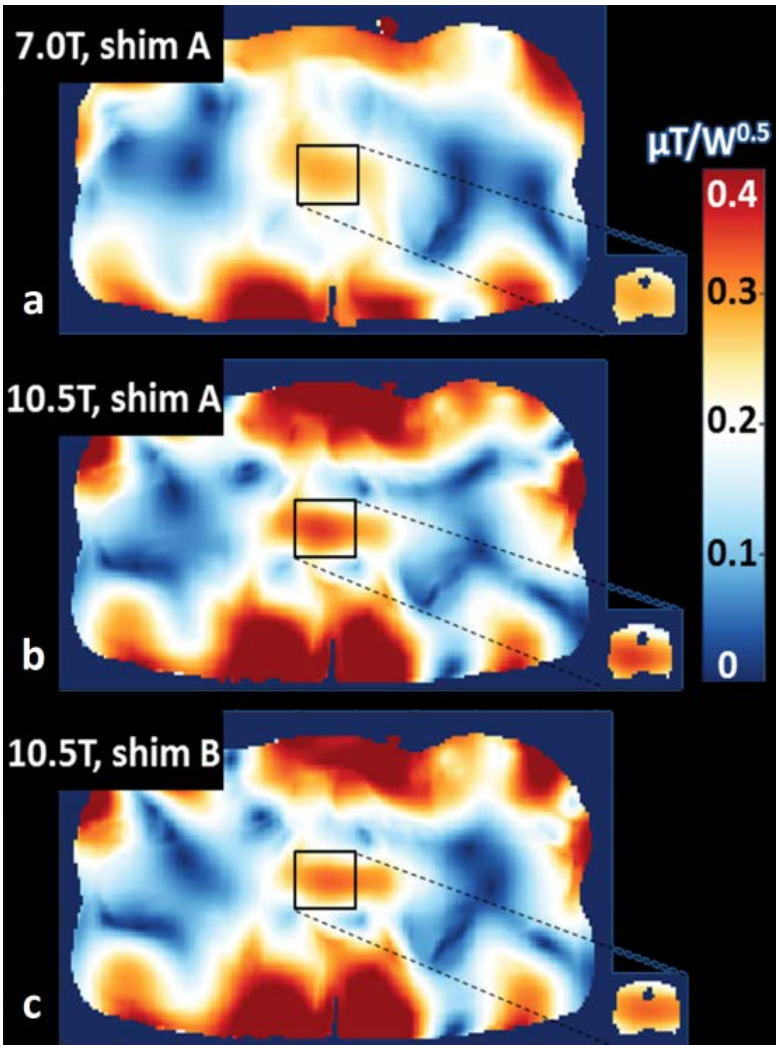

Supporting Figure S1. Simulated power efficiency distributions of phase-only efficiency shim solutions at (a) 7.0 and (b) 10.5 T. (c) Power efficiency distribution of an efficiency – field uniformity tradeoff solution at 10.5 T is shown. These phase-only shim solutions are annotated in Figure 4.

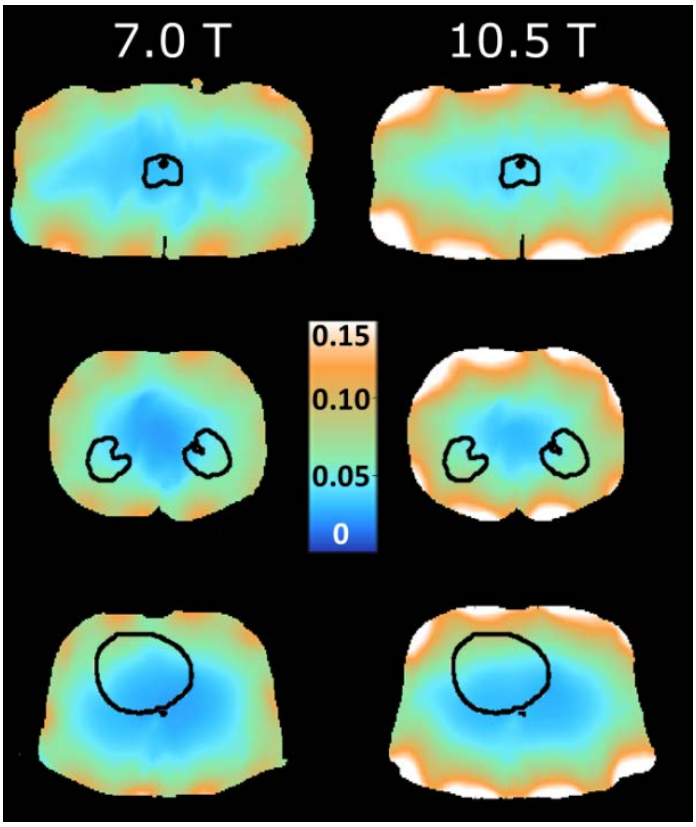

Supporting Figure S2. Numerically computed and RSOS combined B_1^- distributions along axial slices intersecting the prostate (top row), kidneys (middle row) and heart (bottom row) of Duke are shown for the 7.0 T and 10.5 T antenna arrays along left and right columns, respectively.

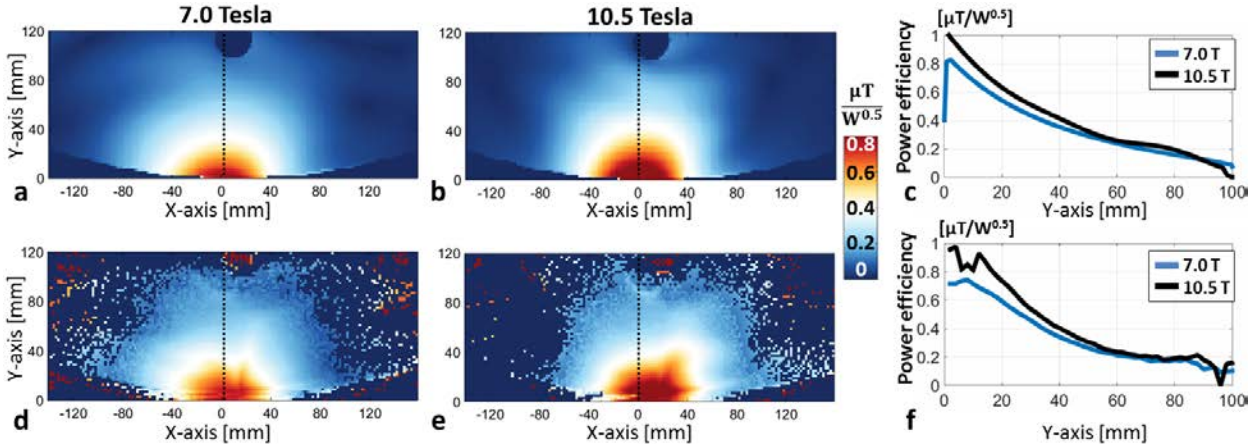

Supporting Figure S3. Simulated and measured power efficiency distributions of single dipole antenna elements are shown along a central axial slice inside a uniform saline phantom in top and bottom rows, respectively. (c) Power efficiency profiles along the annotated lines are plotted from numerical and (f) experimental maps.

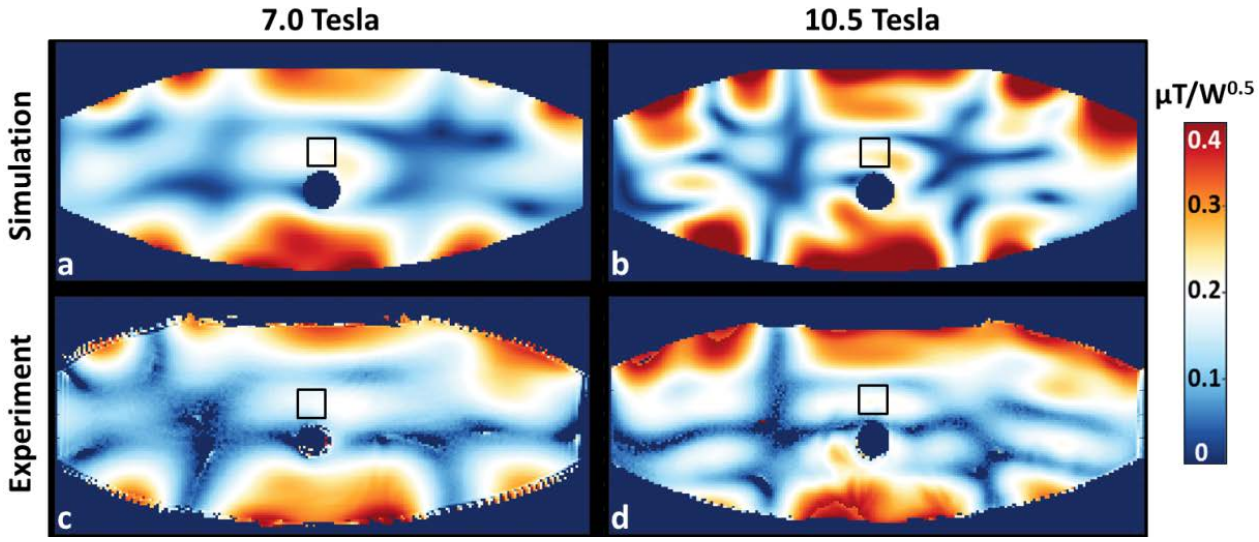

Supporting Figure S4. (a-b) Simulated and (c-d) measured power efficiency distributions at 7.0 and 10.5 tesla are shown. Phase-only efficiency shimming was performed inside annotated regions.

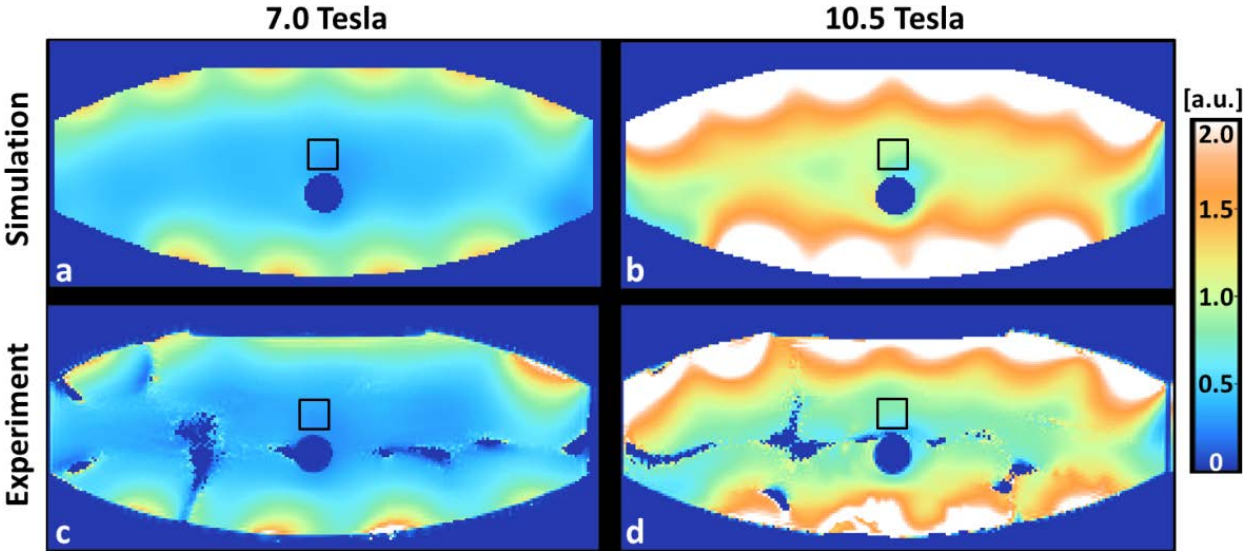

Supporting Figure S5. (a-b) Simulated and (c-d) measured SNR distributions at 7.0 and 10.5 tesla are shown. SNR gains of 2.39- and 2.26-fold are simulated and measured inside the annotated regions, respectively.

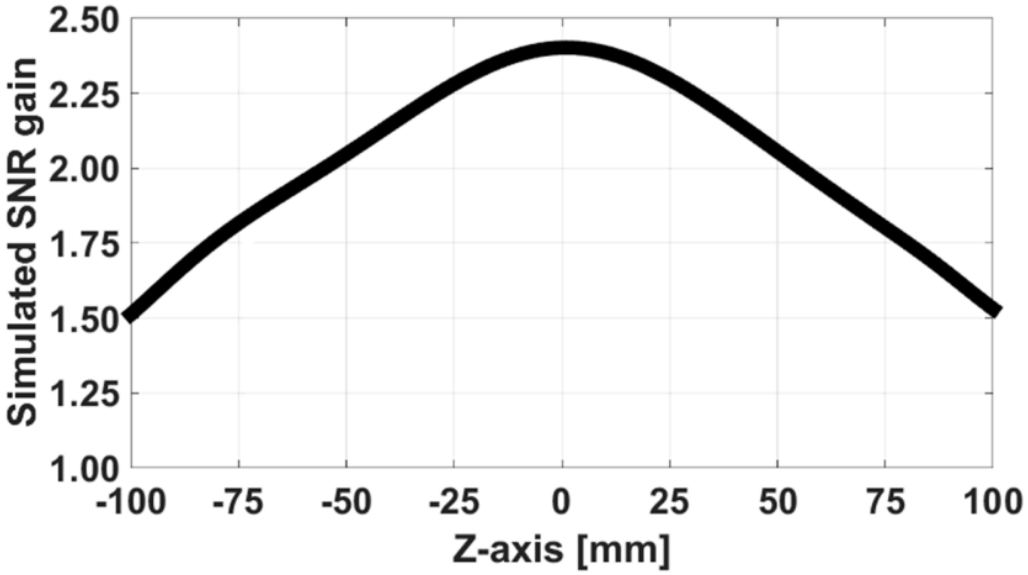

Supporting Figure S6. Numerically computed SNR gain at 10.5 T inside the annotated regions of the torso phantom (Supporting Figure S5) is plotted along z-dimension. More than 2.25-fold gain is observed in a 58 mm-wide region. SNR gains of 2- and 1.5-fold are observed in 110 and 200 mm-wide regions, respectively.